Energy Storage System Utilization, in a Distribution Power System

Dušan Medveď, Ľubomír Beňa, Rikin Jitendrakumar Tailor

Technical University of Košice, Faculty of Electrical Engineering and Informatics, Department of Electric Power Engineering,
Mäsiarska 74, 042 00, Košice, Slovak Republic
Dusan.Medved@tuke.sk, Lubomir.Bena@tuke.sk,
Rikin.Jitendrakumar.Tailor@tuke.sk

Abstract: The contribution of energy storage systems (ESS) to the electricity system is the subject of this paper. There were implemented aspects that are extremely popular and typical in power system setup according to distribution network characteristics. For this reason, a power network included sources like wind farms and solar farms, and in some unfavorable situations, the distribution network link was used as a backup source of electricity. In this power system, load was seen as having constant power. Energy storage systems were put into place throughout the simulation to make up for lost power until a particular stage of discharge, at which point connections to the distribution system (DS) were made. Simulations were carried out in the Matlab/Simulink environment, to examine the collaboration of the aforementioned elements, over a 48-hour period, under various conditions.

Keywords: solar power plant; wind power plant; energy storage system

1   Introduction

Households or companies who produce extra fuel or energy and occasionally supply it to the national (or local) distribution network, while also consuming the same fuel or energy from the network, are considered to be consumers of renewable energy sources (RES) (when their fuel or energy requirements exceed their own production). To do this, households install rooftop PV panels that produce electricity [1-3]. Additionally, these homeowners have the option to use battery storage to increase the amount of PV energy they consume on their own; this practice is called as prosumer in the literature. Businesses that produce biogas and feed it into the gas grid can also do this while using gas from the same grid at various times or in other locations.

The power network may already use such an element to regulate the power in the network if prosumers take part in benefit programs and so give free capacity for the network operator's aims. For this aim, the research discussed in this paper will be applied, in which the prosumer (Energy Storage System (ESS)) [17] [29] is used as a typical storage device and, in the case of a network power loss, the prosumer serves as an energy producer. The Simulink software, which was used to model a variety of potential circumstances in the electrical network, was used to examine the impact of such a prosumer's operation.

2   Simulation of a Case Study

The presented case study concerns the connection of the on-grid electrical network with the distribution system (DS) for the purposes of delivery, or power sales, and vice versa. This connection is made at the 22 kV node (designated M1 in Figure 1). The necessary power is obtained from the DS in the event that there is not enough energy to support the load. This model also includes other sources, including a wind farm (WPP) and a photovoltaic power plant (PVP) [4], [12-15].
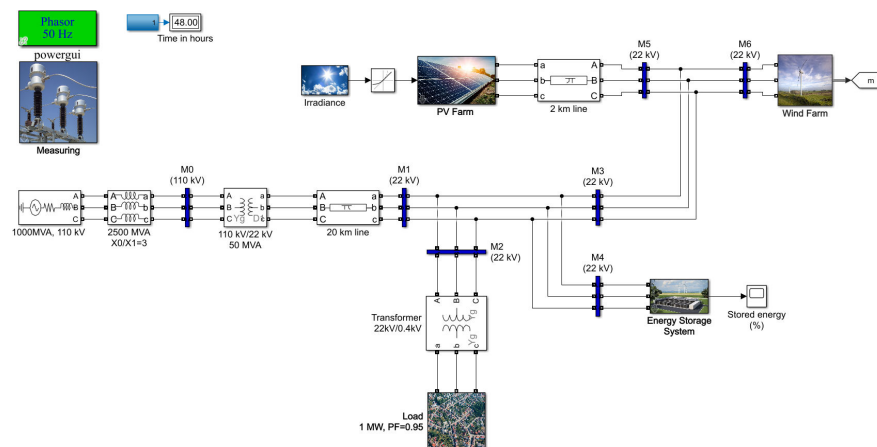

Figure 1

The environment of the Simulink program includes a schematic connection of the electrical circuit

In the distribution system, the M1 node creates the link between the distributor and prosumer. The prosumer is made up of a photovoltaic power plant (PVP), a wind power plant (WPP), and an energy storage system (ESS) at nodes M5 and M6. The measurement site for a load measurement system is also a load measuring at node M2.

The model offers measurements of critical parameters in real-time. In addition to current and active power flow, voltage monitoring in each node, frequency monitoring, and condition monitoring of the SoC (State of Charge) ESS are included.

The model also offers a comparison of the active power of production and non-production units. The identical components used to build the prosumer system depicted in Figure 1 were also used to build these systems.

1.1 The Predetermined Design Parameters

- A photovoltaic power plant (PVP) that is linked and has a total installed capacity of 1800 kWp, a useable area of 12000 m^2 and a 15% efficiency [17] [25]

- The 2-day sun diagram was used to determine the solar radiation properties (Figure 2).
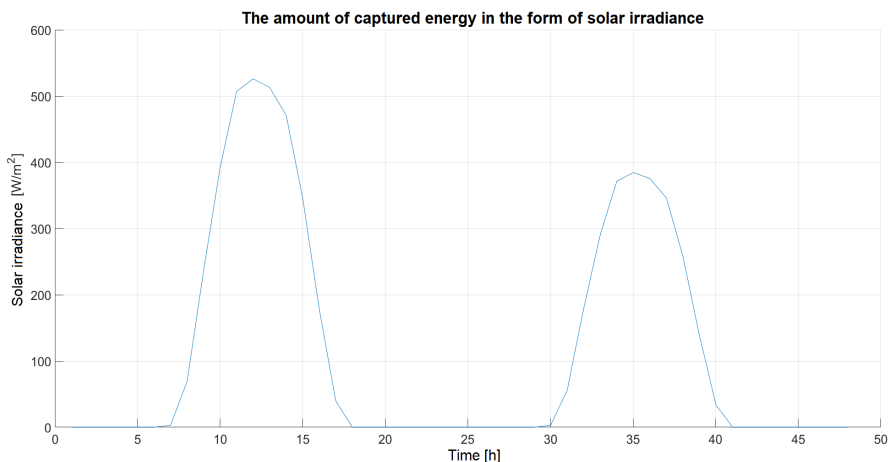

Figure 2

Properties of solar radiation

- A load with a peak power of 1 MW (with the option to attach additional technical devices as a load with a total power of 3×50 kW in case of RES excess power)

- Load characteristics are determined using Figure 3

- The term "ESS" (Energy Storage System) can refer to a variety of potential energy storage technologies, including flywheels, compressed air, supercapacitors, etc.
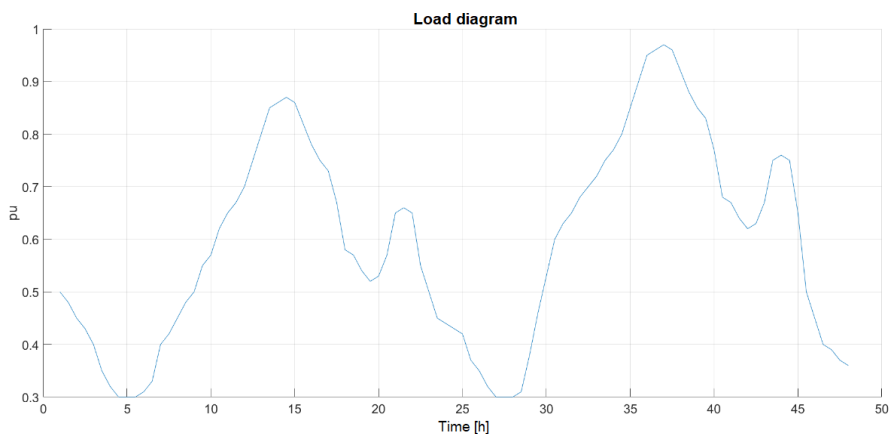
Figure 3

Graph illustrating the load throughout a 48-hour simulation (per units)

- Linked wind power plant with $P_i = 400$ kW at nominal wind speed of $v_{nom} = 9$ m/s

- The set ESS parameters are in accordance with Figure 4, with the exception of parameter no. 5, i.e., the maximum permitted power obtained from the DS has been adjusted from the original 400 kW to 250 kW

The Energy Storage System (ESS), similar to the Battery Energy Storage System (BESS), comprises four components: the control unit (ESS Control), the State of Charge (SoC) status computation, current sources that emulate ESS functionality (similar to a photovoltaic unit), and a 0.4 kV/22 kV transformer (Refer to Figure 4) [24].
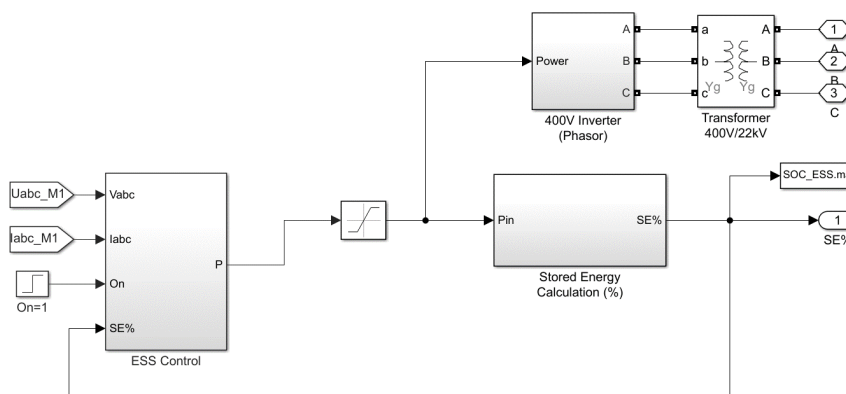

Figure 4

The ESS block subsystem is composed of four integral parts

The ESS, akin to the BESS, gets its charge from the distribution system (DS) during low tariff periods, which in this simulation model are set from 24:00 to 6:00. The system only permits charging when the ESS capacity is under the nominal ESS capacity.

The ESS control block incorporates several variables, including combined voltages and currents in node M1, active power computation, a constant for the maximum active power that can be sourced from the DS, and a constant for the maximum charging power [30].

The control block compares the immediate active power measurement with the maximum allowable active power consumption. Should the prosumer exceed the maximum allowable power consumption from the DS, the control block outputs the difference between the immediate active power value and the maximum permissible active power consumption, leading to the discharge of the ESS. This control function is only valid during the period between regular charging cycles, that is, from 6:00 to 24:00.

The "Charging Logic" block manages the charging behavior, outputting a logical "1" during the designated charging time and comparing it with the SoC state. If the SoC level falls under a set parameter, the ESS initiates charging at a specified interval [20-22].

To accurately simulate the ESS behavior, it is critical to monitor the SoC in real-time, which is accomplished using the Stored Energy Calculation block. The primary purpose of the ESS is to supplement the load when the maximum power consumption from the DS is exceeded.
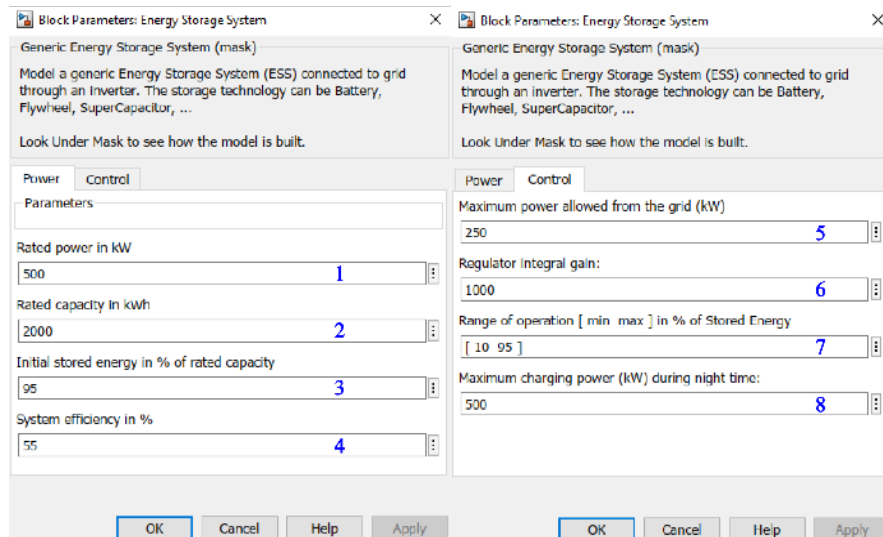

Figure 5
ESS's default settings

Legend (parameters) for Figure 5:

1   Represents rated power in kW

2   Represents nominal ESS capacity in kWh

3   Represents initial ESS capacity in %

4   Represents system efficiency in %

5   Represents the maximum permitted power consumption in kW from the distribution network after which the ESS will start supplying power

6   Represents constant of the integration regulator

7   Represents range of usable battery capacity in %
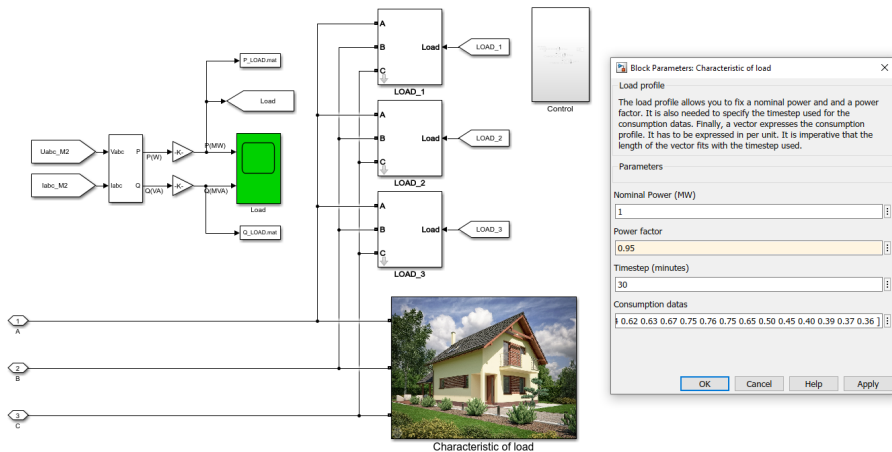
8   Represents maximum charging power in kW

Figure 6

Diagram provides a comprehensive view of the distribution and management of dynamic and static loads within an energy system

The Load Block subsystem, depicted in Figure 6, is bifurcated into two sectors: a dynamic load and a static load.

The dynamic load incorporates the connection of several hundred households, along with the nearby industrial components. This is analogous to a dynamic network where the load varies over time. The static load, on the other hand, represents the technological equipment link, such as multiple electric boilers utilized for Domestic Hot Water (DHW) production. This connection operates in three stages (3×50 kW) when there's a surplus of active power on the side of the prosumer and the asynchronous motor [14].

The subsystem connection of the Load Block is shown in Figure 6. The dynamic load offers the capability to determine the nominal power in megawatts and to adjust the power factor, which influences the magnitude of the reactive power drawn by the load and the load characteristics. All electrical quantities are measured at the M2 node (22 kV), taking transformer losses into consideration.

For dynamic loads, analogous to Photovoltaic (PV) or Energy Storage System (ESS) units, there are current source connections operating on the same principle. However, the regulation of these sources is dependent on the load characteristic, and these sources contribute negative alternating current to the circuit.

3   An Outline of Transients

We took into account the beginning conditions of the model setup and separated the observed time (48 hours) into discrete intervals where we documented the evolution of power, voltage, frequency, and other significant features.
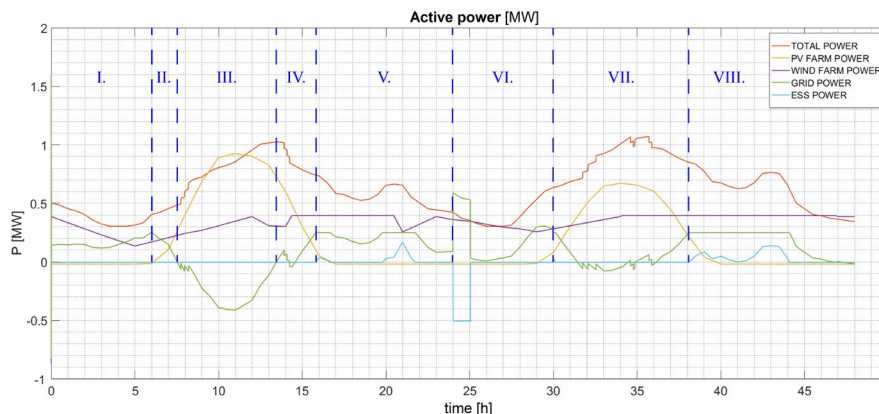

Figure 7
Characteristics of active powers

Fig. 7's active power characteristics are described as follows:

- Power from the wind power plant (WPP) and from the DS is utilized to cover the load in the *I. interval* between 0 and 6 o'clock. ESS has finished charging.

- It begins providing PVP power to the network at the start of *II. interval*, which reduces the amount of power drawn from the DS.

- The extra electricity from RES is given to the DS during the *III. interval* with the intention of selling it. The technological equipment is connected

as a load in three states with a combined power of 3×50 kW if the power supplied to the DS from RES exceeds the value of 50 kW, with the shutdown of technological equipment being coupled not only to the value of power supplied to the DS from RES but also for a specific period of time when they draw power from the network. This indicates that even if the RES does not supply power to the DS, these technological devices can still draw power from the network.

- Because the prerequisites for their continued operation are not satisfied, technical equipment is disconnected during the *IV. interval*.

- It will begin sending ESS power to the network at the start of the *V. interval* since the need of the maximum permitted power taken from the DS, namely 250 kW, has been satisfied.

- The period is set aside for charging the ESS during the *VI. interval*, which lasts between 24. and 30. hours. Even when fully charged to its built-in rated capacity in this time zone, the ESS cannot power the network.

- The wind farm supplies a rated output of 400 kW from around 34. o'clock in *VII. interval*, practically to the end of the simulation, which is characterized by a lower delivery of electricity from PVP than the III. period. Similar to III. interval, technical equipment is linked as a load in the event that there is extra electricity from RES.

- When it is becoming dark and the power from the PVP is fast decreasing in the last *VIII. period*, it is once again turned on by the ESS, which stabilizes the power obtained from the DS at 250 kW. Figure 13's depiction of the ESS SoC shows that the ESS capacity stabilized at 60% SoC. Table 1 shows that WPP, with a total of 16.17 MWh of power delivered to the network over the whole monitored period, was the main supplier, followed by PVP (9.85 MWh). 19.93% of the total power needed to handle the load was used by the prosumer from the DS.

Table 1

Usage of electricity during case simulation

W [MWh]	LOAD	TOTAL	ESS	GRID	PV FARM	WIND FARM
W_{IN_A}*	29.94	0.00	–0.71	–1.54	–0.51	0.0
W_{OUT_A}**	0.00	29.94	0.48	6.19	9.85	16.17

* W_{IN_A} is the electricity consumed by the load, accordingly in the form of losses

** W_{OUT_A} is electricity delivered by production units

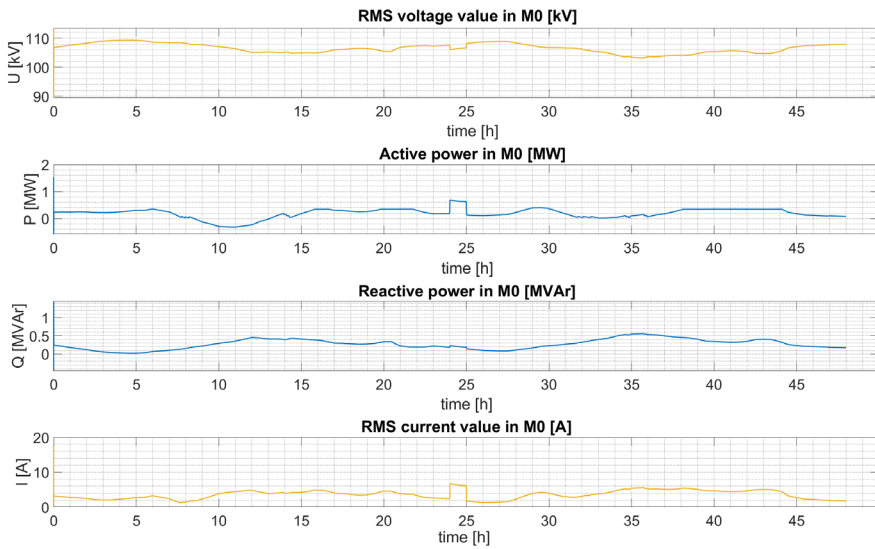The following graphs show the courses of the relevant quantities in nodes M0 to M6.

Figure 8

Electrical parameters that were measured at the M0 node
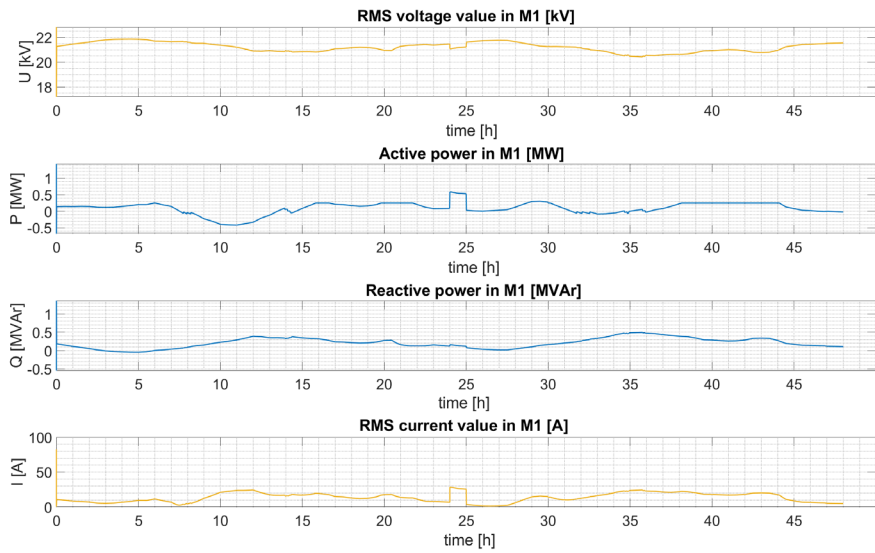
Figure 9

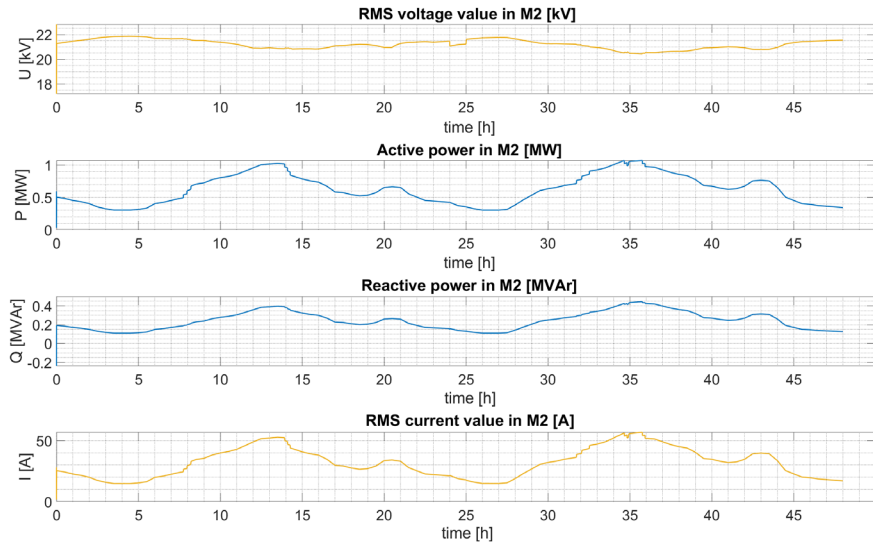Electrical parameters that were measured at the M1 node

Figure 10

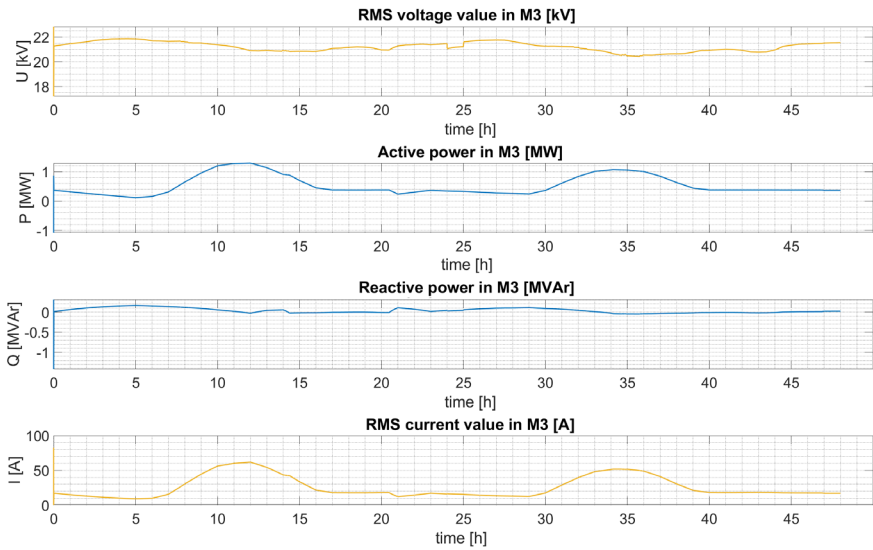Electrical parameters that were measured at the M2 node

Figure 11

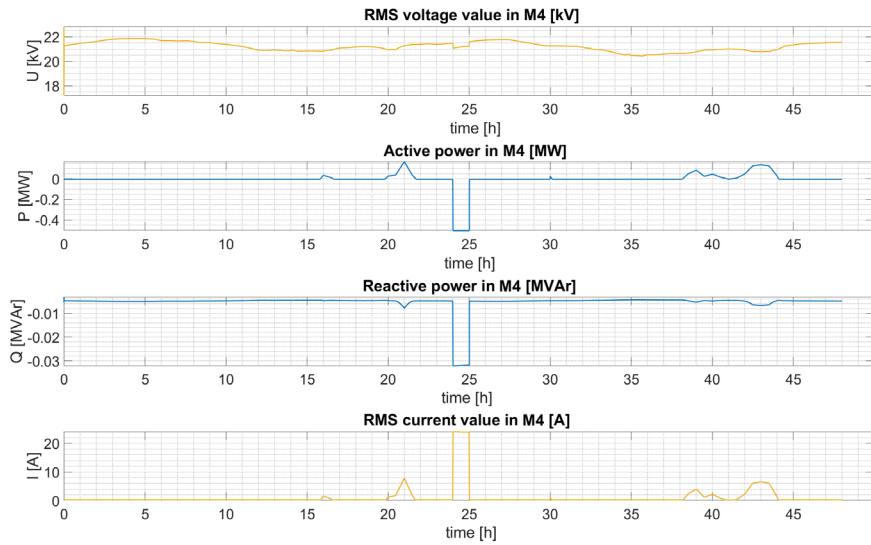Electrical parameters that were measured at the M3 node

Figure 12
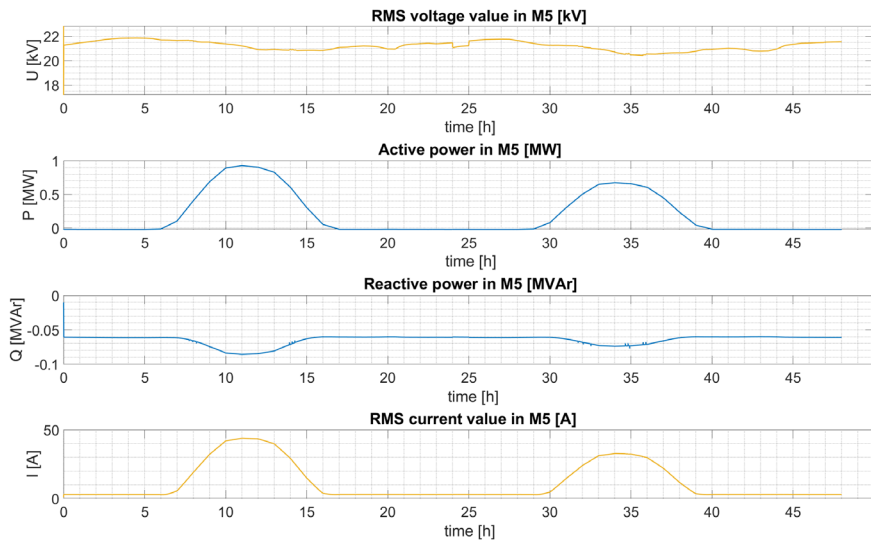Electrical parameters that were measured at the M4 node

Figure 13
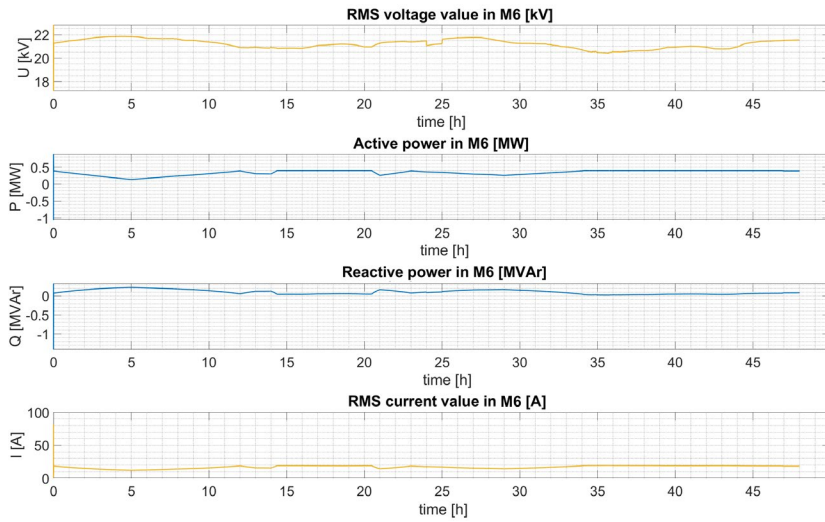Electrical parameters that were measured at the M5 node

Figure 14

Electrical parameters that were measured at the M6 node
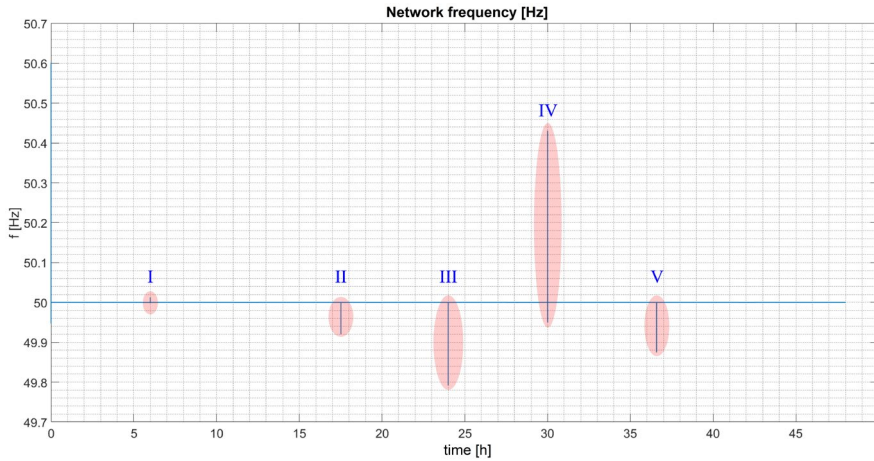

Figure 15

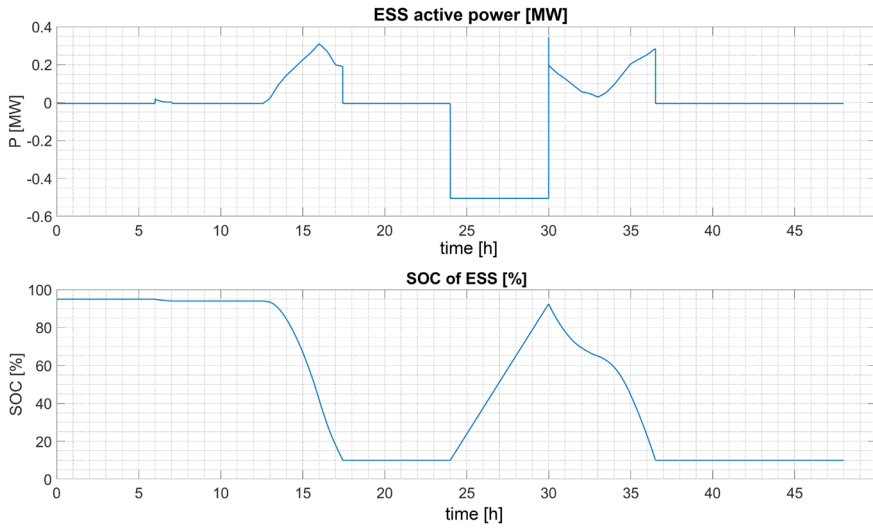The network's frequency fluctuation throughout the measured period

Figure 16

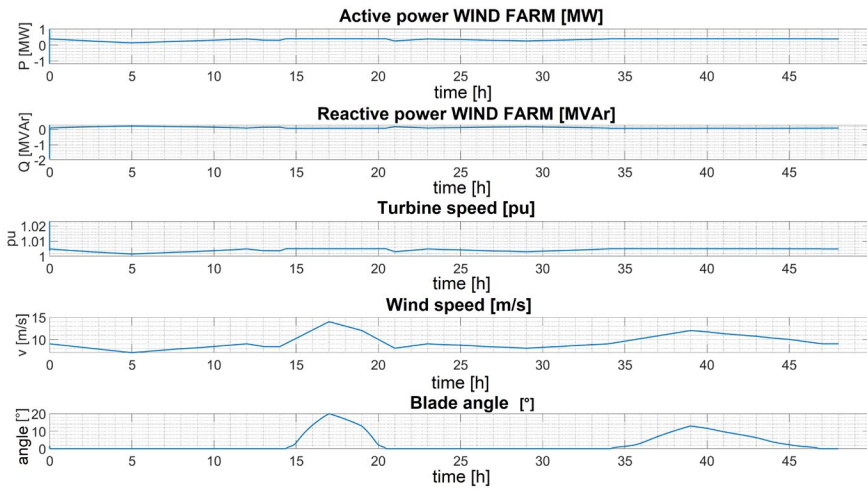The ESS's active power and state of charge state

Figure 17

Wind power plant characteristics that have been observed (blade rotation, wind speed, rotor speed)

The network's frequency characteristics are described in Figure 15:

I.   The progressive connection of the load, or technical equipment, in three stages of 3×50 kW results in a fall in frequency below the nominal value f_n

II.   The gradual disconnection of the load, or technological equipment, results in a rise in frequency above the nominal value f_n

III. The charging of the ESS causes the frequency to fall below the nominal value f_n, and the disconnection of the ESS causes the frequency to rise (end of charge, SoC = 95%)

IV.   The connection of the ESS as a result of the prosumer exceeding the maximum permitted power consumption from the DS, which is 250 kW, causes the frequency to grow over the nominal value f_n

V.   The connection or disconnection of the load, where the regulation was decreased or raised by the power supply from DS, is again the cause of the frequency falling below or rising over the nominal value

Conclusions

In the case scenario, a WPP with an installed power of 400 kW at a wind nominal speed of 9 m/s was added to the prosumer's electrical circuit design. The solar panels' useable area was 12000 m^2, and their efficiency was 15%, increasing the PVP plant's installed capacity to $P_i = 1800$ kWp. The parameter for the ESS, which originally set the maximum permitted power consumption from the DS at 400 kW, was adjusted to 250 kW.

In the case scenario, an extra active power demand in the form of technical equipment (such as an electric boiler) was connected in three stages of 3×50 kW, which resulted in the consumption of 29.94 MWh of electricity within the allowed time period. Direct usage of RES electricity to meet the load accounted for 80.07% of the total (23.97 MWh). Also included in the extra RES electricity sent to the DS was a volume totaling 1.54 MWh.

When evaluating the quality of the electricity according to STN 50160 for LV and MV, we can determine that there were no dangerous phenomena in the entire interconnected electricity network when the load or production unit was connected or disconnected, respectively, and that the voltages and frequencies, the two key quality indicators, were kept within acceptable bounds. According to the frequency characteristics, the power control frequency errors for the on-grid system were in the order of tenths and did not exceed 0.5 Hz.

Acknowledgement

References

[1] J. Dang, J. Seuss, L. Suneja, R. G. Harley, "*SOC feedback control for wind and ESS hybrid power system frequency regulation*", In Proceedings of the IEEE Power Electronics and Machines in Wind Applications, Denver, CO, USA, 16-18 July 2012; pp. 1-7, doi: 10.1109/PEMWA.2012.6316384

[2] G. S. Lakshmi, O. Rubanenko, A. Hunko, "*Control of the Sectioned Electrical Network Modes with Renewable Energy Sources*", In Proc. of the 2021 International Conference on Sustainable Energy and Future Electric Transportation (SEFET), Hyderabad, India, 21-23 January 2021; pp. 1-6, doi: 10.1109/SeFet48154.2021. 9375781

[3] G. Ren, "*MATLAB/Simulink-Based Simulation and Experimental Validation of a Novel Energy Storage System to a New Type of Linear Engine for Alt. Energy Vehicle Applications*", IEEE Trans. Power Electron. 2018, 33, 8683-8694, doi: 10.1109/TPEL.2017. 2784563

[4] M. Makhlouf, F. Messai, K. Nabti, H. Benalla, "*Modeling and simulation of grid-connected photovoltaic distributed generation system*", In Proceedings of the 2012 First International Conference on Renewable Energies and Vehicular Technology, Nabeul, Tunisia, 26-28 March 2012; pp. 187-193, doi: 10.1109/REVET.2012.6195269

[5] N. K. Roy, H. R. Pota, "*Current status and issues of concern for the integration of distributed generation into electricity networks*", IEEE Syst. J. 2014, 9, 933-944, doi: 10.1109/JSYST.2014.2305282

[6] B. Dolník, et.al., "*The Response of a Magnetic Fluid to Radio Frequency Electromagnetic Field*". In: Acta Physica Polonica A. doi: 10.12693/APhysPolA.131.946

[7] I. Kolcunová, et. al., "*Experimental observation of negative differential characteristic of corona discharge in ultraviolet spectrum*". In: Journal of Electrostatics. doi: 10.1016/j.elstat.2016.12.016

[8] J. Zbojovský, L. Kruželák, M. Pavlík, "*Impedance Spectroscopy of Liquid Insulating Materials*". In: IEEE CANDO-EPE 2018, IEEE International Conference and Workshop in Óbuda on Electrical and Power Engineering, Nov. 20-21, 2018, Budapest, Hungary. ISBN: 978-1-7281-1154-4

[9] M. Pavlík, I. Kolcunová, L. Lisoň, "*Measuring the shielding effectiveness and reflection of electromagnetic field of building material*". In: 2015 16th International Scientific Conference on Electric Power Engineering (EPE), 2015, pp. 56-59, doi: 10.1109/EPE.2015.7161186

[10] I. Kolcunová, J. Zbojovský, M. Pavlík, S. Bucko, J. Labun, M. Hegedus, M. Vavra, R. Cimbala, J. Kurimský, B. Dolník, J. Petráš, J. Džmura, "*Shielding Effectiveness of Electromagnetic Field by Specially Developed Shielding Coating*". In: Acta Physica Polonica A. Warsaw (Poland):

Instytut Fizyki. Vol. 137, No. 5 (2020), pp. 711-713. ISSN 0587-4246. doi: 10.12693/APhysPolA.137.711

[11] J. Jirinec, D. Rot, R. Velev, "*The Energy Efficient Solution for Intelligent Lighting*", In: 2019 20th International Scientific Conference on Electric Power Engineering (EPE), 2019, pp. 1-4, doi: 10.1109/EPE.2019.8777938

[12] K. Noháč, L. Raková, V. Mužik, K. Máslo, "*Open Source Platforms for Dynamic Stability Assessment*", In: 2019 20th International Scientific Conference on Electric Power Engineering (EPE), 2019, pp. 1-6, doi: 10.1109/EPE.2019.8778087

[13] D. Kapral, P. Bracinik, M. Roch, M. Hoger, "*Optimization of distribution network operation based on data from smart metering systems*", In: Electrical Engineering, Vol. 99, Issue 4, Springer, New York, USA, 2017, December, pp: 1417-1428, ISSN 0948-7921. doi: 10.1007/s00202-017-0628-x

[14] Z. Eleschova, B. Cintula, V. Volcko, A. Belan, J. Bendik, M. Cenky, "*The Influence of Smart Grids on a Large Synchronous Generators Operation*", In: Proceedings of the 2018 19th International Scientific Conference on Electric Power Engineering (EPE), pp 43-48, doi: 10.1109/EPE.2018.8395948

[15] K. Nohac, M. Tesarova, L. Nohacova, J. Veleba, V. Majer, "*Utilization of Events Measured by WAMS-BIOZE-Detector for System Voltage Stability Evaluation*", In: IFAC Workshop on Control of Transmission and Distribution Smart Grids (CTDSG), Volume: 49, Issue: 27, pp 364-369, ISSN 2405-8963, doi: 10.1115/1.4043103

[16] D. Rot, J. Kozeny, S. Jirinec, J. Jirinec, A. Podhrazky, I. Poznyak, "*Induction melting of aluminium oxide in the cold crucible*", In: 18th International Scientific Conference on Electric Power Engineering (EPE) 2017, pp 1-4, doi: 10.1109/EPE.2017.7967281

[17] D. Pál, Ľ. Beňa, J. Urbanský, M. Oliinyk, "*The impact of reconfiguration on power losses in smart networks*", In: 2020 21st International Scientific Conference on Electric Power Engineering (EPE), 2020, pp. 1-5, doi: 10.1109/EPE51172.2020.9269189

[18] M. Sulír, J. Porubän, "*Augmenting Source Code Lines with Sample Variable Values*", In: 2018 IEEE/ACM 26th International Conference on Program Comprehension (ICPC), 2018, pp. 344-347, doi: 10.1145/3196321.3196364

[19] M. Tesařová, R. Vykuka, "*Impact of Distributed Generation on Power Flows Along Parallelly Operated MV Feeders*", In: Int. Conf. on Env. and El. Eng. and 2018 IEEE Ind. and Com. Power Syst. Europe, EEEIC/I and CPS Europe 2018, doi: 10.1109/EEEIC.2018.8493640

[20]   P. Girovský, J. Žilková, J. Kaňuch, "*Optimization of Vehicle Braking Distance Using a Fuzzy Controller*". In: Energies. 2020; 13(11):3022. doi: 10.3390/en13113022

[21]   M. Bereš, D. Kováč, T. Vince, I. Kováčová, J. Molnár, I. Tomčíková, J. Dziak, P. Jacko, B. Fecko, Š. Gans, "*Efficiency Enhancement of Non-Isolated DC-DC Interleaved Buck Converter for Renewable Energy Sources*". In: Energies. 2021; 14(14):4127. doi: 10.3390/en14144127

[22]   B. Cintula, Ž. Eleschová, M. Cenký, P. Janiga, J. Bendík, A. Beláň, "*Three-Phase and Single-Phase Measurement of Overhead Power Line Impedance Evaluation*". In: Energies. 2021; 14(19):6314. doi: 10.3390/en14196314

[23]   J. Kanuch, P. Girovsky, "*The device to measuring of the load angle for salient-pole synchronous machine in education laboratory*", In: Measurement, Volume 116, 2018, pp 49-55, ISSN 0263-2241, doi: 10.1016/j.measurement.2017.10.043

[24]   M. Cenký, J. Bendík, Ž. Eleschová, A. Beláň, B. Cintula, P. Janiga, "*Probabilistic Model of Electric Vehicle Charging Demand to Distribution Network Impact Analyses*", In: 2019 20th International Scientific Conference on Electric Power Engineering (EPE), 2019, pp. 1-6, doi: 10.1109/EPE.2019.8777973

[25]   B. C. Sánchez, M. Váry, M. Perný, F. Janíček, V. Šály, J. Packa, "*Prediction and production of small PV power plant*", In: 2017 18th International Scientific Conference on Electric Power Engineering (EPE), 2017, pp. 1-5, doi: 10.1109/EPE.2017.7967276

[26]   M. Pavlik, "Compare of shielding effectiveness for building materials," Przeglad Elektrotechniczny, 95(5), 137-140, doi: 10.15199/48.2019.05.33

[27]   S. Bucko, M. Krchnak, R. Cimbala, L. Kruzelak, J. Zbojovsky, "*Abrasive properties of transformer oil-based magnetic nanofluid*," In: 19th International Scientific Conference on Electric Power Engineering (EPE), 2018, pp. 1-4, doi: 10.1109/EPE.2018.8396038

[28]   A. Beláň, B. Cintula, M. Cenký, P. Janiga, J. Bendík, Ž. Eleschová, A. Šimurka, "*Measurement of Static Frequency Characteristics of Home Appliances in Smart Grid Systems*". Energies 2021, 14, 1739. doi: 10.3390/en14061739

[29]   M. Kajanova, P. Bracinik, "*Social welfare-based charging of electric vehicles in the microgrids fed by renewables*" In: International Journal of Electrical Power & Energy Systems, Vol. 138, doi: 10.1016/j.ijepes.2022.107974

[30]   P. Jacko, M. Beres, I. Kovacova, J. Molnar, T. Vince, J. Dziak, B. Fecko, S. Gans, D. Kovac, "*Remote IoT Education Laboratory for Microcontrollers Based on the STM32 Chips*", In: Sensors. 2022; 22(4):1440. doi: 10.3390/s2204144

[31]   M. Beres, D. Kovac, T. Vince, I. Kovacova, J. Molnar, I. Tomcikova, J. Dziak, P. Jacko, B. Fecko, S. Gans, "*Efficiency Enhancement of Non-Isolated DC-DC Interleaved Buck Converter for Renewable Energy Sources*", Energies. 2021; 14(14):4127. doi: 10.3390/en14144127